The KCNQ1-KCNE2 K^+ channel is required for adequate thyroid I^- uptake

Kerry Purtell,* Monika Paroder-Belenitsky,[†] Andrea Reyna-Neyra,[†,1] Juan P. Nicola,[‖] Wade Koba,[‡] Eugene Fine,[‡] Nancy Carrasco,[†,§,1] and Geoffrey W. Abbott*,[2]

*Department of Pharmacology, Weill Cornell Medical College, New York, New York, USA; [†]Department of Molecular Pharmacology, [‡]M. Donald Blaufox MicroPET Laboratory for Molecular Imaging, Department of Radiology, and [§]Department of Biochemistry, Albert Einstein College of Medicine, Bronx, New York, USA; and [‖]Department of Cellular and Molecular Physiology, Yale School of Medicine, New Haven, Connecticut, USA

ABSTRACT **The KCNQ1 α subunit and the KCNE2 β subunit form a potassium channel in thyroid epithelial cells. Genetic disruption of KCNQ1-KCNE2 causes hypothyroidism in mice, resulting in cardiac hypertrophy, dwarfism, alopecia, and prenatal mortality. Here, we investigated the mechanistic requirement for KCNQ1-KCNE2 in thyroid hormone biosynthesis, utilizing whole-animal dynamic positron emission tomography. The KCNQ1-specific antagonist (−)-[3*R*,4*S*]-chromanol 293B (C293B) significantly impaired thyroid cell I^- uptake, which is mediated by the Na^+/I^- symporter (NIS), *in vivo* (*dSUV/dt*: vehicle, 0.028±0.004 min^{-1}; 10 mg/kg C293B, 0.009±0.006 min^{-1}) and *in vitro* (EC_{50}: 99±10 μM C293B). Na^+-dependent nicotinate uptake by SMCT, however, was unaffected. *Kcne2* deletion did not alter the balance of free *vs.* thyroglobulin-bound I^- in the thyroid (distinguished using ClO_4^-, a competitive inhibitor of NIS), indicating that KCNQ1-KCNE2 is not required for Duox/TPO-mediated I^- organification. However, *Kcne2* deletion doubled the rate of free I^- efflux from the thyroid following ClO_4^- injection, a NIS-independent process. Thus, KCNQ1-KCNE2 is necessary for adequate thyroid cell I^- uptake, the most likely explanation being that it is prerequisite for adequate NIS activity.—Purtell, K., Paroder-Belenitsky, M., Reyna-Neyra, A., Nicola, J. P., Koba, W., Fine, E., Carrasco, N., Abbott, G. W. The KCNQ1-KCNE2 K^+ channel is required for adequate thyroid I^- uptake. *FASEB J.* 26, 3252–3259 (2012). www.fasebj.org**

Key Words: hypothyroidism · Kv7.1 · MiRP1 · positron emission tomography · sodium/iodide symporter

POTASSIUM ION (K^+) CHANNELS provide a K^+-selective aqueous pore for the diffusion of K^+ across the plasma membrane and are essential for the function of most, if not all, mammalian cell types. Voltage-gated potassium (K_v) channels are gated (opened and closed) by changes in membrane potential. They are opened by membrane depolarization and are essential for the timely repolarization of excitable cells. Other K^+ channels are constitutively active, that is, open at resting membrane potential. Defining the role of constitutively active K^+ channels *in vivo* can be challenging: they contribute an often temporally invariant "background" K^+ conductance and may be expressed in cell types resistant to faithful primary culturing or direct electrophysiological analysis. In addition, constitutively active K^+ channels, in particular, may be important for processes difficult to quantify *in vivo* or *in vitro*, including ion homeostasis and hormone synthesis and release.

The KCNQ1-KCNE2 potassium channel has an unusual molecular composition for a constitutively active K^+ channel but is widely studied because its subunits are required for a range of processes essential in human physiology. The KCNQ1 pore-forming (α) subunit contains the S4-based voltage-sensing domain present in voltage-gated K^+, Na^+, and Ca^{2+} channels. However, although homomeric channels formed by a tetramer of KCNQ1 α subunits are voltage-gated, heteromeric channel complexes comprising KCNQ1 together with the single-transmembrane segment KCNE2 β subunit are constitutively active, and relatively voltage-insensitive (1). KCNQ1-KCNE2 channels are essential for the physiology of at least two types of nonexcitable, polarized epithelial cells: gastric parietal cells, which secrete gastric acid, and thyroid epithelial cells, which secrete thyroid hormones. Targeted deletion of either *Kcnq1* or *Kcne2* causes both hypothyroid-

Abbreviations: 2D, 2-dimensional; 3D, 3-dimensional; C293B, (−)-[3*R*,4*S*]-chromanol 293B; CT, computed tomography; HA, hemagglutinin; MMI, methimazole; NIS, Na^+/I^- symporter; PET, positron emission tomography; SMCT, sodium/monocarboxylate transporter; SUV, standardized-uptake value; Tg, thyroglobulin; TPO, thyroid peroxidase

[1] Current address: Department of Cellular and Molecular Physiology, Yale School of Medicine, New Haven, CT 06519, USA.

[2] Correspondence and current address: University of California, Irvine, School of Medicine, Department of Pharmacology, 356A Med Surge II, Zot Code: 4625, Irvine, CA 92697, USA. E-mail: abbottg@uci.edu

doi: 10.1096/fj.12-206110

0892-6638/12/0026-3252 © FASEB

ism and achlorhydria, demonstrating the absolute necessity for both α and β subunits in the native channel complex (2–6).

Kcne2$^{-/-}$ mice also exhibit dwarfism, alopecia (**Fig. 1*A***), prenatal mortality, and cardiomegaly, all of which arise from their underlying hypothyroidism (5). Human *KCNQ1* and *KCNE2* gene mutations cause potentially fatal ventricular and atrial cardiac arrhythmias, probably primarily due to the role of these subunits in cardiac myocyte K^+ currents (7, 8); however, the discovery of the KCNQ1-KCNE2 channel in mouse and human thyroid suggests a possible endocrine component to these electrical disturbances (5). Here, we sought to elucidate the mechanistic basis for the requirement for KCNQ1-KCNE2 channels in thyroid function. To examine thyroid physiology *in vivo*, we utilized positron emission tomography (PET), which facilitated real-time quantification of $^{124}I^-$ fluxes *in vivo*, in mice genetically and pharmacologically manipulated to isolate different steps in thyroid hormone biosynthesis. We demonstrate that KCNQ1-KCNE2 is required for Na^+/I^- symporter (NIS)-mediated thyroid cell uptake of I^-, an essential step in thyroid hormone biosynthesis.

MATERIALS AND METHODS

Transgenic mouse generation, care, and use

We generated and genotyped the C57BL/6 *Kcne2*$^{-/-}$ mouse line, as described previously (4, 5) and housed and used mice, according to the U.S. National Institutes of Health Guide for the Care and Use of Laboratory Animals. Animal procedures were approved by the Animal Care and Use Committees at Weill Medical College of Cornell University and Albert Einstein College of Medicine.

PET and computed tomography (CT)

Mice were secured to a bed with a breathing tube over their snout that provided a continuous supply of isoflurane anesthetic throughout the imaging procedure (Fig. 1*C*). Imaging

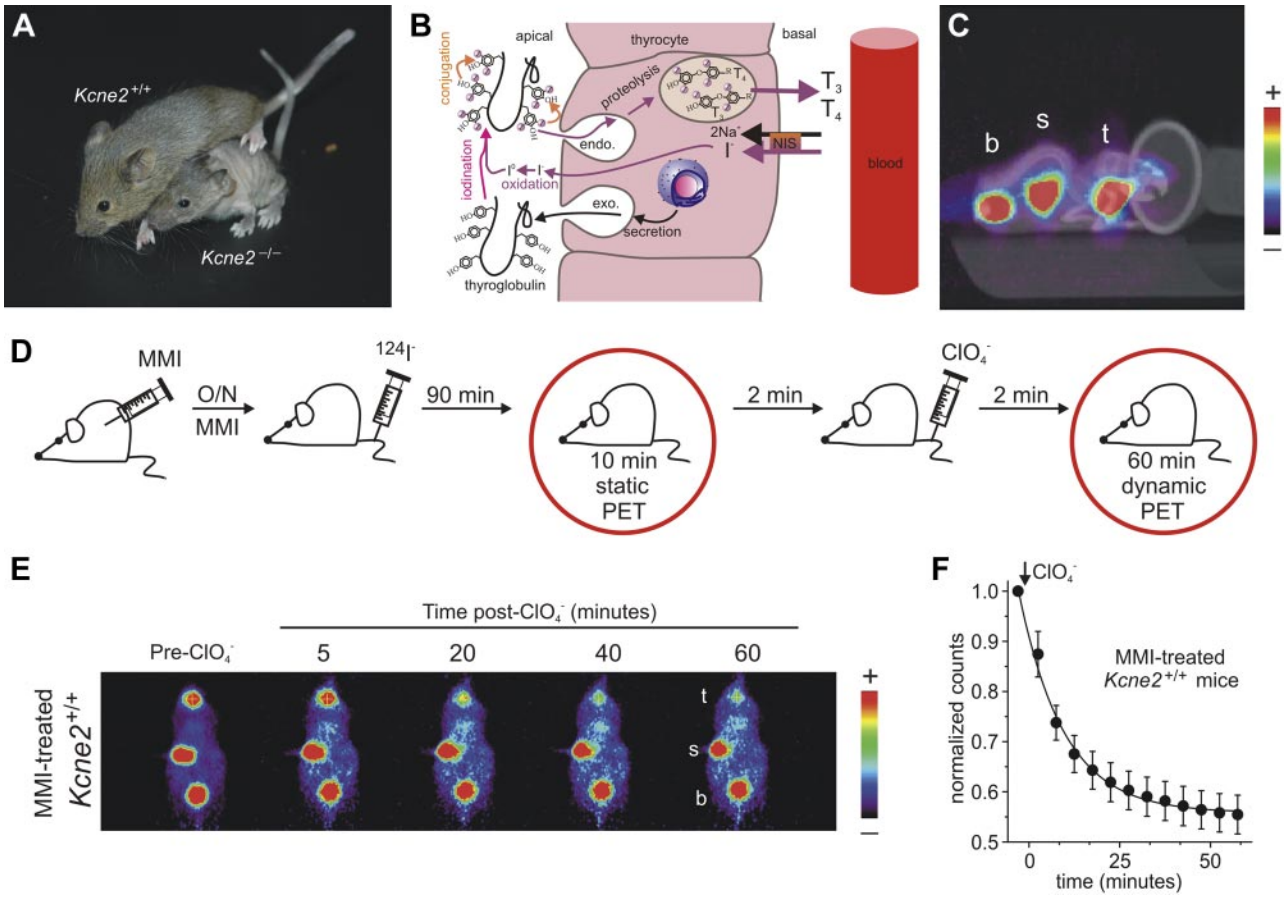

Figure 1. PET quantification of ClO_4^--induced $^{124}I^-$ discharge in MMI-treated mice. *A*) Age-matched 3-wk-old *Kcne2*$^{+/+}$ and *Kcne2*$^{-/-}$ pups bred from same-genotype dams, showing dwarfism and alopecia in the latter. *B*) Schematic of I^- uptake and organification in the thyroid. *C*) Exemplar coregistered PET-CT image of a 6-mo-old *Kcne2*$^{+/+}$ mouse, injected with $^{124}I^-$ and positioned in the anesthesia-delivery nose cone. Heat map (scale at right) for PET image shows positioning of the thyroid (t), stomach (s), and bladder (b). CT bony structures are evident in purple color scale. *D*) Schematic showing experimental protocol for validating PET imaging of ClO_4^--induced I^- discharge, using MMI-pretreated mice. *E*) Exemplar pre- and post-ClO_4^- PET images for an MMI-pretreated *Kcne2*$^{+/+}$ mouse (protocol in *D*; 150 μCi of $^{124}I^-$ injected). Tissues labeled as in *C*. Scale bar at right. *F*) Mean thyroid counts normalized to pre-ClO_4^- thyroid counts for MMI-pretreated *Kcne2*$^{+/+}$ mice, demonstrating ClO_4^- -induced $^{124}I^-$ discharge (protocol in *D*; n=5). Error bars = SEM.

was performed on an Inveon Multimodality scanner (Siemens, Munich, Germany), in which CT X-rays were generated by an 80-kV peak voltage difference between cathode and tungsten target at 0.5-mA current and 250-ms exposure time. The CT field of view was 5.5 by 8.5 cm, with an overall resolution without magnification of 100 μm. Subsequent PET imaging was performed by translating the test subject on the imaging gantry into the PET device, which provided a 12.7-cm axial and 10-cm transaxial active field of view. The PET scanner has no septa, and acquisitions were performed in 3-dimensional (3D) list mode. A reconstructed full-width half-maximum resolution of <1.4 mm is achievable in the center of the axial field of view. List mode acquisition of data was performed to permit dynamic reframing for kinetic evaluation of $^{124}I^-$ uptake, where indicated. After each acquisition, data were sorted into 3D sinograms, and images were reconstructed using a 2-dimensional (2D)-ordered subset expectation maximization algorithm. Data were corrected for deadtime counting losses, random coincidences, and the measured nonuniformity of detector response (*i.e.*, normalized), but not for attenuation or scatter. After both acquisitions, CT images were coregistered with PET images using a previously stored linear transformation matrix.

Analysis was performed using ASIPRO (Siemens) dedicated software. All image studies were inspected visually in a rotating 3D projection display to examine for interpretability and image artifact. Manual regions of interest (ROIs) were defined around the thyroid. Successive scrolling through 2D slices (each 1.2 mm thick in the axial images) permitted measurement of a radioactivity within defined volumes and also as profiles in reconstructed image planes. The counts per cubic centimeter within this volume multiplied by the 3D ROI volume after correction for detector sensitivity, animal weight, and time of injection determined the standardized-uptake value (SUV). For quantitative comparisons of I^- efflux rates *in vivo* during ClO_4^- discharge, we fitted SUV decay over time with a single exponential function and reported the rate as τ. For quantitative comparison of I^- uptake, we subjected initial (linear) portion of individual uptake plots (0–13.3 min) to linear regression analysis, and we report the slope as mean *dSUV/dt,* as described previously (9).

Methimazole (MMI) treatment

Mice were given an intraperitoneal injection of 1 mg MMI (Sigma-Aldrich, St. Louis, MO, USA) in 100 μl total volume filter-sterilized PBS, and overnight *ad libitum* access to drinking water containing 250 μg/ml MMI.

Perchlorate discharge assay

Lactating dams, anesthetized with 1.5% isoflurane-oxygen mixture, received 200–300 μCi (7–12 MBq) $^{124}I^-$ in 0.1 ml saline solution *via* tail-vein injection. Dams were placed back in their cages for 90 min to allow accumulation of the $^{124}I^-$ tracer in the thyroid, then imaged for 10 min before, and for the 60 min following, injection of 2-mg sodium perchlorate ($NaClO_4$; Sigma Aldrich) in a total volume of 0.1 ml PBS *via* tail vein. Measurements of thyroid counts taken at 5-min intervals following $NaClO_4$ injection were normalized to the maximum count value taken from the pre-ClO_4^- image.

Uptake experiments

Stock solutions of 80 mM (−)-[3*R*,4*S*]-chromanol 293B (C293B; Tocris Biosciences, Cambridge, UK) dissolved in pure DMSO were prepared and stored at −20°C. The stock was diluted to a final concentration of 2.5 mg/ml in PBS with 20% DMSO. Vehicle controls contained 20% DMSO in PBS. Mice were injected with 0.1 ml of drug or vehicle 30 min before injection with $^{124}I^-$ (150 μCi, 5.55 MBq) dissolved in 0.1 ml saline.

Cell culture, transport, and flow cytometry experiments

FRTL-5 cells were grown in Coon's modified Ham's F12 medium supplemented with 5% newborn calf serum (Sigma Aldrich) and 6 different hormones (10 mg/ml insulin 5 mg/ml , transferrin, 10 nM hydrocortisone, 10 nt/ml tripeptide Gly-L-His-L-Lys, 0.3 mU/ml TSH, and 10 ng/ml somatostatin) in a water-saturated atmosphere of 5% CO_2 and 95% air at 37°C. For transport assays, FRTL-5 cells were cultured on 24-well plates.

Uptake experiments were initiated by adding 500 μl HBSS (137 mM NaCl, 5.4 mM KCl, 1.3 mM $CaCl_2$, 0.4 mM $MgSO_4$, 0.4 mM $Na_2HPO_4{\cdot}7H_2O$, 0.44 mM KH_2PO_4, and 0.55 mM glucose), buffered with 10 mM HEPES-KOH (pH 7.5) containing 20 μM $Na^{125}I^-$ (Perkin Elmer, Wellesley, MA, USA) with a specific activity of 50 Ci/mol, in the presence or absence of C293B. FRTL-5 cells were incubated at 37°C in a humidified atmosphere for 30 min. Reactions were terminated by aspirating the radioactive solution and washing 3 times with HBSS. Accumulated $^{125}I^-$ was determined by permeabilizing cells with ethanol for 20 min and quantifying the released radioisotope in a γ counter. Data were standardized per microgram of DNA in each well. Concentration of DNA was assessed by the diphenylamine method (10). [^{14}C]nicotinate (Moravek Biochemicals, Brea, CA, USA) uptake was measured using the same procedure, except that cells were incubated with buffered HBSS containing 50 μM [^{14}C]nicotinate. NaCl was replaced with equimolar concentrations of choline chloride to determine the Na^+ dependence of sodium/monocarboxylate transporter (SMCT)-mediated nicotinate transport.

For flow cytometry, FRTL-5 cells were transduced with extracellular N-terminal hemagglutinin (HA)-tagged human NIS, as described previously (11). Paraformaldehyde-fixed cells were incubated in PBS containing 0.2% BSA with 3 nM anti-HA (clone 3F10) rat monoclonal IgG (Roche Applied Science, Mannheim, Germany). The fluorescence of 2×10^4 cells/tube was assayed in FACSCalibur flow cytometer (BD Biosciences, San Jose, CA, USA). Data were analyzed with FlowJo software (Tree Star, Ashland, OR, USA).

COS-7 cells were grown in DMEM supplemented with 10% heat-inactivated FBS (Sigma-Aldrich). Cells were transfected with 10 μg/10-cm dish pcDNA3.1-rNIS or -hNIS cDNA constructs using polyethylenimine. I^- uptake activity was assayed at 48 h post-transfection.

RESULTS

PET imaging of a chemically induced iodine organification defect in mouse thyroid

We previously utilized PET imaging to discover that *Kcne2* deletion in mice impairs thyroid $^{124}I^-$ accumulation (5). Here, we combined PET with other techniques to determine the underlying mechanism for this impairment. Thyrocytes actively take up I^- *via* NIS at the basolateral surface (12). I^- next effluxes across the thyrocyte apical membrane to the cell-colloid interface, where it is oxidized and covalently incorporated into specific tyrosyl residues on thyroglobulin (Tg; Fig.

1*B*)—a process termed "organification" and catalyzed by thyroid peroxidase (TPO) and the NADPH-dependent H_2O_2-generating system (Duox). Iodinated Tg is then stored in the colloid until demand for thyroid hormones causes Tg to be apically endocytosed and proteolyzed, and thyroid hormones to be basolaterally secreted into the bloodstream (13, 14). To establish the mechanism for impaired thyroid I^- accumulation in *Kcne2*$^{-/-}$ mice, we needed to distinguish between free I^- and iodine covalently incorporated into Tg, and also between I^- uptake and iodine organification, both of which determine thyroid I^- accumulation.

First, we employed coregistered PET and X-ray CT on mice tail-vein-injected with ^{124}I, to confirm positioning of the thyroid signal compared to other I^--accumulating tissues, such as the stomach and bladder (Fig. 1*C*). We then sought to determine whether KCNQ1-KCNE2 is required for thyroid I^- organification, using PET in combination with the well-established perchlorate (ClO_4^-) discharge assay (PDA). ClO_4^-, a competitive inhibitor of NIS that is translocated electroneutrally (15), causes a rapid reduction of free I^- in the thyroid (as I^- can efflux from but not enter the thyrocyte in its presence). When organification is normal, ClO_4^- elicits only moderate thyroid I^- discharge (~15%) because most I^- is rapidly covalently bound to Tg, whereas an organification defect can result in a ClO_4^--induced I^- discharge of 50% or more (16).

We first assessed the suitability of PET for quantifying ClO_4^- discharge in the mouse thyroid, by ascertaining the effect of pretreating wild-type C57BL/6 mice with MMI, a thionamide that blocks I^- organification by inhibiting TPO (17, 18). MMI pretreatment involved an intraperitoneal injection of MMI, followed by overnight *ad libitum* access to water supplemented with MMI. The following day, 90 min after tail-vein injection of $^{124}I^-$, a 10-min static PET image was generated to measure peak $^{124}I^-$ accumulation. Mice immediately received ClO_4^- *via* tail-vein injection and were PET imaged dynamically at 5-min intervals for 60 min (Fig. 1*D*, *E*). Mean thyroid radioactivity at each 5-min interval following ClO_4^- injection was normalized to the mean pre-ClO_4^- thyroid radioactivity to quantify discharge. ClO_4^- resulted in a 45 ± 4% discharge of ^{124}I within the first hour after injection in MMI-pretreated mice, thereby confirming successful detection of the chemically induced organification defect and validating the PET assay (n=5; Fig. 1*F*).

KCNQ1-KCNE2 is not required for I^- organification

We next quantified the effect of targeted deletion of *Kcne2* on ClO_4^--induced discharge of thyroid I^- in non-MMI-treated lactating C57BL/6 mice using PET, following the protocol outlined in **Fig. 2*A***, and observed 19 ± 3% discharge within the first hour after injection in *Kcne2*$^{+/+}$ mice, compared to 14 ± 4% in *Kcne2*$^{-/-}$ mice (n=5; P=0.19; Fig. 2*B*, *C*). There was, therefore, no significant effect of *Kcne2* deletion on organification. Furthermore, both non-MMI-pretreated groups exhibited significantly less I^- discharge than

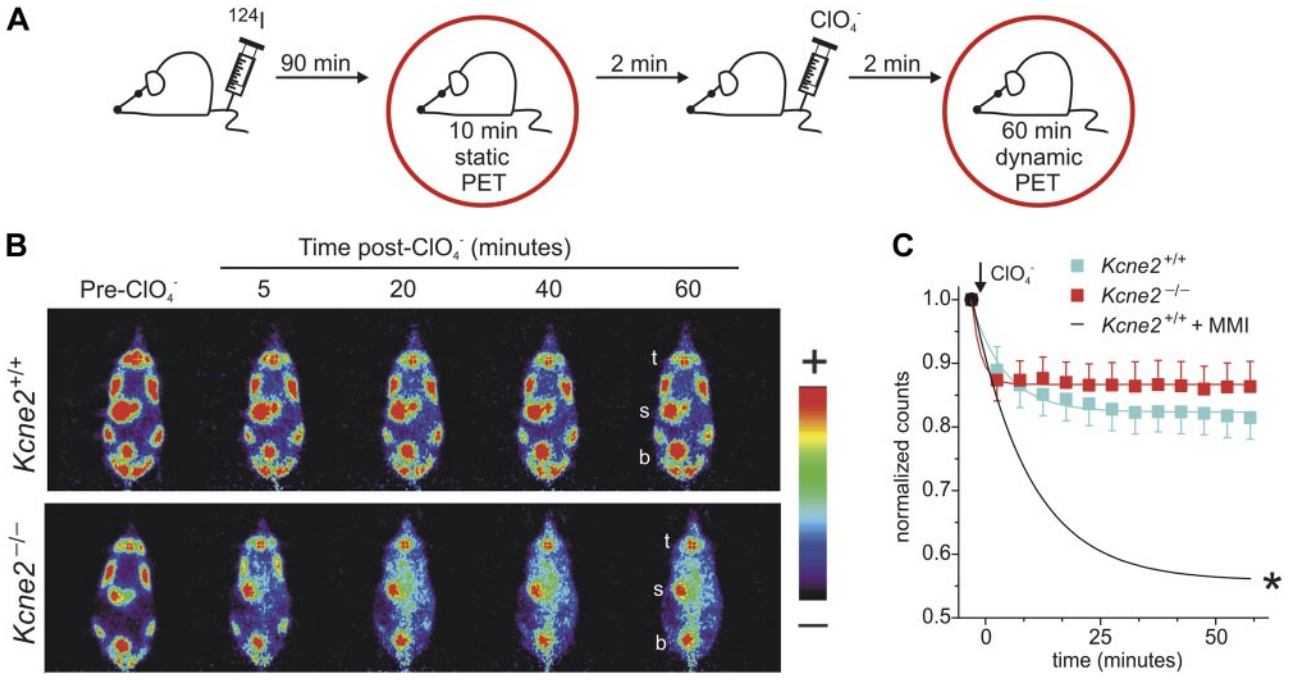

Figure 2. *Kcne2* deletion does not cause an I^- organification defect. *A*) Schematic showing experimental protocol for PET quantification of ClO_4^--induced I^- discharge in *Kcne2*$^{+/+}$ and *Kcne2*$^{-/-}$ mice. *B*) Exemplar pre- and post-ClO_4^- PET images for *Kcne2*$^{+/+}$ and *Kcne2*$^{-/-}$ mice (protocol in *A*). Labeled tissues: thyroid (t), stomach (s), and bladder (b). Scale bar at right. *C*) Mean thyroid counts normalized to pre-ClO_4^- thyroid counts for *Kcne2*$^{+/+}$ and *Kcne2*$^{-/-}$ mice as in *B*, compared to data for MMI-pretreated *Kcne2*$^{+/+}$ mice (data from Fig. 1*F*); n = 5 mice/group. Error bars = SEM. *$P < 0.0005$ *vs.* non-MMI-pretreated mice, 60-min time point.

MMI-pretreated *Kcne2*$^{+/+}$ mice (n=5; P<0.0005; Fig. 2*C*). Interestingly, while the extent of I^- efflux following ClO_4^- injection appeared *Kcne2*-independent, fitting the discharge plots from individual mice with a single exponential function indicated a trend (P=0.17) toward increased rate of I^- efflux in *Kcne2*$^{-/-}$ mice (τ=284±117 ms; n=5) compared to their *Kcne2*$^{+/+}$ counterparts (712±366 ms; n=4). Lactating mice were used for these experiments because hypothyroidism in *Kcne2*$^{-/-}$ mice is most marked during early development, gestation, lactation, and in old age (5).

KCNQ1-KCNE2 is required for efficient I^- uptake

The absence of an organification defect in *Kcne2*$^{-/-}$ mice, combined with our previous finding that *Kcne2* deletion impairs thyroid I^- accumulation (5), suggested KCNQ1-KCNE2 could be important for NIS-mediated I^- uptake. To test this hypothesis, we first used the highly specific KCNQ1 antagonist (−)-[3R,4S]-chromanol 293B (C293B) to acutely inhibit KCNQ1-KCNE2, in *Kcne2*$^{+/+}$ mice pretreated with MMI to inhibit organification, allowing us to assess I^- transport at steady state. This approach dissociated the uptake process from $^{124}I^-$ organification, eliminating radiolabeling of Tg and thus facilitating exclusive imaging of NIS-mediated transport of free $^{124}I^-$ in the thyroid. Following overnight MMI treatment, mice were tail-vein injected with either C293B (10 mg/kg) or vehicle, then 30 min later tail-vein injected with $^{124}I^-$ and immediately dynamically PET imaged for 60 min to quantify $^{124}I^-$ uptake (**Fig. 3*A***). Strikingly, C293B (10 mg/kg) impaired $^{124}I^-$ by 42% at 60 min, giving a mean thyroid radioactivity of 0.69 ± 0.11 SUV (*i.e.*, counts normalized to whole-body mean radioactivity concentration; whole-body SUV=1.00, by definition) compared to 1.18 ± 0.06 SUV in vehicle-injected mice (n=5; P<0.005; Fig. 3*B, C*), signifying inhibition of ^{124}I uptake and retention. Initial thyroid I^- uptake rates were reduced 3-fold by C293B (10 mg/kg), with the *dSUV/dt* being reduced from 0.028 ± 0.004 min^{-1} (vehicle) to 0.009 ± 0.006 min^{-1} (C293B; n=5, P=0.014; Fig. 3*D*).

To validate this finding in an alternative system, we performed $^{125}I^-$ flux assays using the highly functional rat thyroid-derived FRTL-5 nonpolarized cell line (**Fig. 4*A***), which we previously showed expresses KCNQ1-KCNE2 channel protein and K^+ current (5). FRTL-5 cells exhibit minimal I^- organification, but express NIS and efficiently transport I^-. Increasing concentrations of C293B inhibited NIS-mediated I^- uptake in a dose-dependent manner (EC_{50}: 99±10 μM C293B; n=4; Fig. 4*B*); in contrast, they did not affect another Na^+-driven transport process, namely SMCT-mediated nicotinate uptake (Fig. 4*B*), demonstrating the specificity of the inhibition of I^- uptake and also indicating that impaired NIS function arising from KCNQ1-KCNE2 inhibition does not stem from a dis-

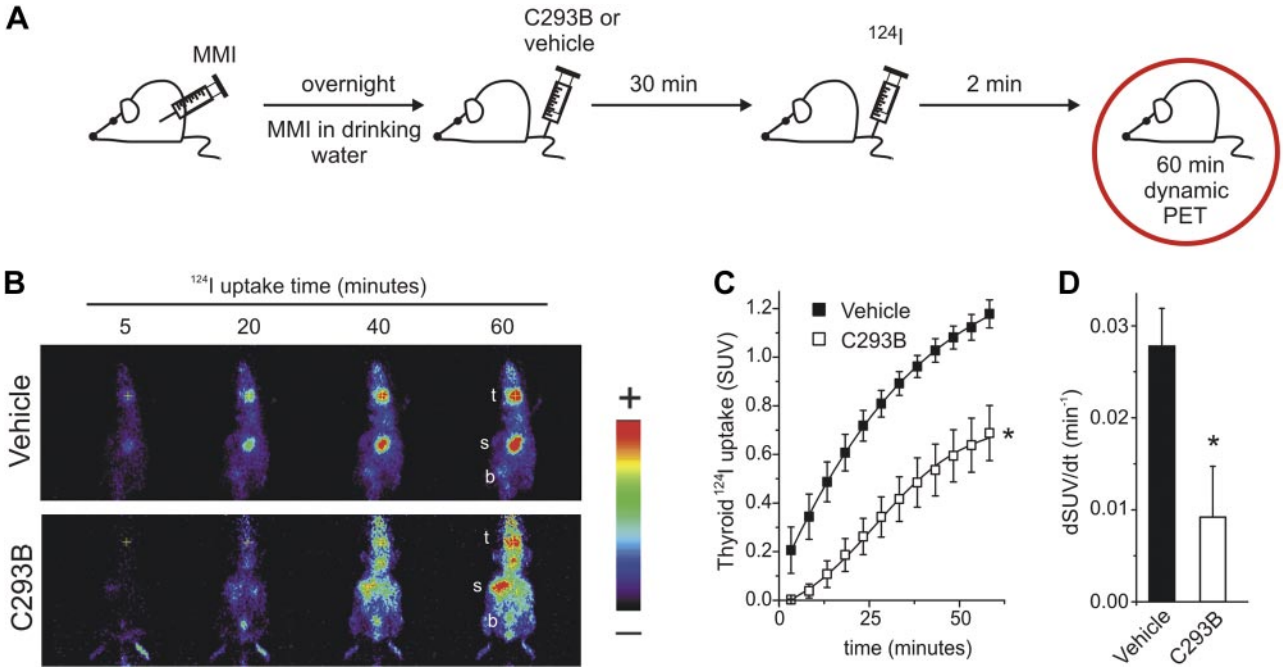

Figure 3. Pharmacological inhibition of KCNQ1-KCNE2 impairs thyroid I^- uptake *in vivo*. *A*) Schematic showing experimental protocol for PET quantification of the effect of C293B (10 mg/kg) on thyroid $^{124}I^-$ uptake in MMI-pretreated *Kcne2*$^{+/+}$ mice. *B*) Exemplar PET images for vehicle- or 10 mg/kg C293B-treated *Kcne2*$^{+/+}$ mice, at the indicated times following $^{124}I^-$ injection (protocol in *A*). Labeled tissues: thyroid (t), stomach (s), and bladder (b). Scale bar at right. *C*) Mean thyroid $^{124}I^-$ counts during the first hour following $^{124}I^-$ injection for MMI-pretreated *Kcne2*$^{+/+}$ mice as in *B*, injected with vehicle or 10 mg/kg C293B 30 min before $^{124}I^-$; n = 5 mice/group. Error bars = SEM. *P < 0.005 *vs.* vehicle-treated, 60-min time point. *D*) Mean initial (0–13.3 min) thyroid I^- uptake rates determined from graphs as in *C* for individual mice, groups as in *C*; n = 5. *P = 0.014.

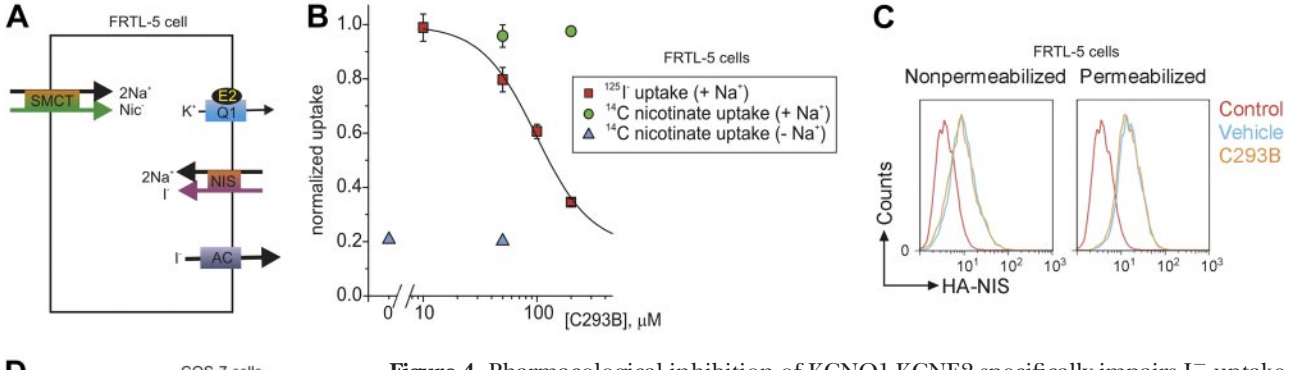

Figure 4. Pharmacological inhibition of KCNQ1-KCNE2 specifically impairs I^- uptake *in vitro*. *A*) FRTL-5 cell simplified model to illustrate various key ion fluxes. AC, anion channel; E2, KCNE2; Q1, KCNQ1; Nic^-, nicotinate; NIS, Na^+/I^- symporter; SMCT, sodium/monocarboxylate transporter. *B*) C293B inhibition of $^{125}I^-$ steady-state uptake by FRTL5 cells (red squares) for various C293B concentrations. Values were normalized to steady-state uptake of $^{125}I^-$ by FRTL5 cells bathed in DMSO as a vehicle control. Data are means of 4 independent experiments/concentration, each performed in triplicate. $^{125}I^-$ uptake values in the presence of ClO_4^- were <3.7% (data not shown). Dose response was fitted with a sigmoidal function. Also shown: [^{14}C]nicotinate steady-state uptake in FRTL-5 cells bathed in medium containing 50 μM [^{14}C]nicotinate, and either Na^+ (green circles) or choline (blue triangles), to assess effects of C293B on the function of SMCT. *C*) FRTL-5 cells expressing extracellular HA-tagged NIS were incubated with 100 μM C293B or vehicle for 1 h. Histograms indicate NIS expression at the plasma membrane quantified by flow cytometry using an anti-HA antibody under nonpermeabilized conditions (left) or permeabilized conditions as a control for total protein (right). Unstained control cells in red, DMSO-treated cells in cyan, and C293B-treated cells in orange. Data are representative of 2 experiments, each performed in duplicate. *D*) I^- steady-state uptake in rNIS- or hNIS-transfected COS-7 cells incubated with 20 μM $^{125}I^-$, 100 μM C293B, or vehicle as indicated, and in the absence (red) or presence (blue) of 40 μM ClO_4^-. Data are representative of 3 independent experiments, each performed in triplicate. Error bars = SD.

rupted Na^+ gradient. In support of the KCNQ1-dependence of action of C293B, it did not inhibit cell-surface expression of HA-tagged NIS in FRTL-5 cells, as quantified by flow cytometry, indicating that the decrease of I^- uptake caused by C293B is not due to fewer NIS molecules at the plasma membrane (Fig. 4*C*). Likewise, C293B had no effect on I^- uptake through rat or human NIS when heterologously expressed, without KCNQ1 overexpression, in COS-7 cells (Fig. 4*D*).

DISCUSSION

After initially being recognized for their respective roles in voltage-dependent K^+ channels in cardiac myocytes, KCNQ1 and KCNE2 were found to form a constitutively active K^+ channel (1), subsequently identified in gastric parietal cells (3, 19). KCNQ1-KCNE2 recycles K^+ from the parietal cell to the stomach lumen, facilitating the 1:1 exchange of H^+ ions for K^+ ions required by the H^+/K^+-ATPase for gastric acid secretion (3, 19, 20). Thus, genetic disruption of either *Kcnq1* or *Kcne2* in mice causes achlorhydria and gastric hyperplasia owing to an inability to secrete gastric acid (2, 4). Following up on our recent discovery that the KCNQ1-KCNE2 K^+ channel is important for thyroid hormone biosynthesis (5), we have now used PET to uncover the mechanistic basis for this requirement: without functional KCNQ1-KCNE2, I^- uptake into the thyroid is impaired, with no direct effect on I^- organification (**Fig. 5**).

The requirement for KCNQ1-KCNE2 for thyroidal I^- uptake may indicate that KCNQ1-KCNE2 is necessary for adequate function of NIS, the primary thyrocyte I^- uptake conduit. This functional requirement almost certainly does not involve a need for KCNQ1-KCNE2 to supply the thyrocyte basolateral Na^+/K^+ATPase with K^+, so that it can maintain a Na^+ gradient for NIS, because KCNQ1 inhibition did not affect function of another Na^+-driven transporter, SMCT (Fig. 4*B*).

One possible mechanism is that KCNQ1-KCNE2 is required to regulate thyrocyte membrane potential *in vivo*, and that with *Kcne2* or *Kcnq1* deleted, or the channel pharmacologically inhibited, this function is perturbed. NIS-mediated I^- uptake is electrogenic, with 2 Na^+ entering for every I^-; therefore, its activity would depolarize the cell in the absence of other regulatory ion fluxes. Given that KCNQ1-KCNE2 is constitutively active, it has the capacity to permit K^+ efflux to help maintain a negative membrane potential. If this channel is pharmacologically blocked (Fig. 5*B*), or if the *Kcnq1* gene itself is deleted, the thyrocyte could become depolarized, and NIS function could, therefore, be impaired as a result of a decrease in the membrane potential, one of the two components of the electrochemical driving force of NIS.

Deletion of *Kcne2* may have slightly different effects, albeit still resulting in impaired thyroid hormone biosynthesis. We recently found that KCNE2 is expressed in the choroid plexus epithelium, where it forms K^+ channels with KCNQ1 and with Kv1.3 (KCNA3; ref. 21).

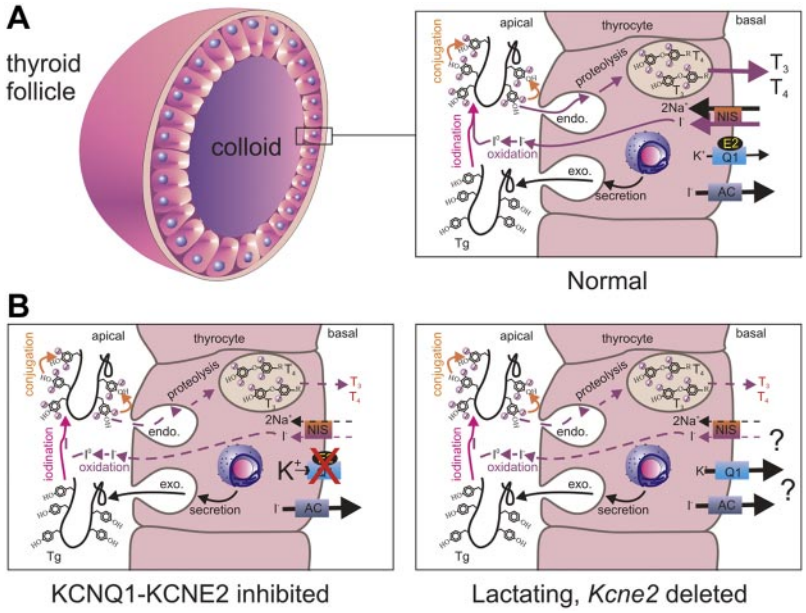

Figure 5. Summary of effects of KCNQ1-KCNE2 disruption on thyrocyte function. *A*) In the normal thyroid, basolateral uptake through NIS supplies I^- for apical organification (iodination of Tg) and thyroid hormone biosynthesis. KCNQ1-KCNE2 is expressed on the basolateral surface. *B*) Left panel: when KCNQ1-KCNE2 is pharmacologically inhibited, organification is not directly impaired, but I^- uptake is reduced, reducing thyroid hormone biosynthesis, while SMCT function is maintained. Right panel: *Kcne2* deletion also reduces I^- uptake without affecting organification. Impaired NIS function is the prime candidate, but it is possible that *Kcne2* deletion also increases I^- leak through anion channels, as suggested by an increased rate of I^- efflux following NIS inhibition by ClO_4^- *in vivo*.

When *Kcne2* is deleted, choroid plexus epithelial outward K^+ currents actually increase, because KCNE2 normally partially suppresses Kv1.3 and KCNQ1 outward currents (although endowing the latter with the ability to remain open at very negative potentials). This hyperpolarizes the choroid plexus cells and may contribute to the higher cerebrospinal fluid [Cl^-] that we observe in *Kcne2*$^{-/-}$ mice (21). It is possible that this effect also occurs in the thyroid of *Kcne2*$^{-/-}$ mice, potentially favoring I^- loss through nonspecific anion channels. Significantly, the loss of I^- from the thyrocyte, which is clearly observed following competitive inhibition of NIS with ClO_4^-, occurs *via* a NIS-independent mechanism, probably through one or more types of anion channel and down the I^- electrochemical gradient. *Kcne2* deletion appeared to increase the rate of this I^- efflux (Fig. 2*C*), and we speculate that thyrocyte I^- "leak" arising from hyperpolarization in *Kcne2*$^{-/-}$ mice could contribute to their inability to accumulate I^- as efficiently as their wild-type counterparts. Future studies will be aimed at further dissecting the molecular basis of the requirement for KCNQ1-KCNE2 in NIS-mediated I^- uptake.

In summary, we demonstrate here that state-of-the-art imaging techniques can be combined with genetically tractable small animal models, pharmacological tools, and in this case a standard clinical assay for I^- organification deficiency (the ClO_4^- discharge test) to discern physiologically and pathophysiologically important mechanisms *in vivo*. The discovery of this link between a K^+ channel and a plasma membrane transporter suggests that similar such links may yet be found in a wide variety of cell types. The findings also present proof-of-principle that pharmacological inhibition of KCNQ1-KCNE2 can be used to alter thyroid function—opening up potential novel therapeutic avenues for thyroid disorders. FJ

This work was supported by U.S. National Institutes of Health grants HL079275 (G.W.A.), DK41544 (N.C.), T32GM073546 (K.P.), and 5T32GM002788 (M.P.B.); American Heart Association grant 0855756D (G.W.A.); and an Irma T. Hirschl Career Scientist Award (G.W.A.).

REFERENCES

1. Tinel, N., Diochot, S., Borsotto, M., Lazdunski, M., and Barhanin, J. (2000) KCNE2 confers background current characteristics to the cardiac KCNQ1 potassium channel. *EMBO J.* **19,** 6326–6330
2. Lee, M. P., Ravenel, J. D., Hu, R. J., Lustig, L. R., Tomaselli, G., Berger, R. D., Brandenburg, S. A., Litzi, T. J., Bunton, T. E., Limb, C., Francis, H., Gorelikow, M., Gu, H., Washington, K., Argani, P., Goldenring, J. R., Coffey, R. J., and Feinberg, A. P. (2000) Targeted disruption of the Kvlqt1 gene causes deafness and gastric hyperplasia in mice. *J. Clin. Invest.* **106,** 1447–1455
3. Grahammer, F., Herling, A. W., Lang, H. J., Schmitt-Graff, A., Wittekindt, O. H., Nitschke, R., Bleich, M., Barhanin, J., and Warth, R. (2001) The cardiac K^+ channel KCNQ1 is essential for gastric acid secretion. *Gastroenterology* **120,** 1363–1371
4. Roepke, T. K., Anantharam, A., Kirchhoff, P., Busque, S. M., Young, J. B., Geibel, J. P., Lerner, D. J., and Abbott, G. W. (2006) The KCNE2 potassium channel ancillary subunit is essential for gastric acid secretion. *J. Biol. Chem.* **281,** 23740–23747
5. Roepke, T. K., King, E. C., Reyna-Neyra, A., Paroder, M., Purtell, K., Koba, W., Fine, E., Lerner, D. J., Carrasco, N., and Abbott, G. W. (2009) Kcne2 deletion uncovers its crucial role in thyroid hormone biosynthesis. *Nat. Med.* **15,** 1186–1194
6. Frohlich, H., Boini, K. M., Seebohm, G., Strutz-Seebohm, N., Ureche, O. N., Foller, M., Eichenmuller, M., Shumilina, E., Pathare, G., Singh, A. K., Seidler, U., Pfeifer, K. E., and Lang, F. (2011) Hypothyroidism of gene-targeted mice lacking Kcnq1. *Pflügers Arch.* **461,** 45–52
7. Wang, Q., Curran, M. E., Splawski, I., Burn, T. C., Millholland, J. M., VanRaay, T. J., Shen, J., Timothy, K. W., Vincent, G. M., de Jager, T., Schwartz, P. J., Toubin, J. A., Moss, A. J., Atkinson, D. L., Landes, G. M., Connors, T. D., and Keating, M. T. (1996) Positional cloning of a novel potassium channel gene: KVLQT1 mutations cause cardiac arrhythmias. *Nat. Genet.* **12,** 17–23
8. Abbott, G. W., Sesti, F., Splawski, I., Buck, M. E., Lehmann, M. H., Timothy, K. W., Keating, M. T., and Goldstein, S. A. (1999) MiRP1 forms IKr potassium channels with HERG and is associated with cardiac arrhythmia. *Cell* **97,** 175–187

9. Beaulieu, S., Kinahan, P., Tseng, J., Dunnwald, L. K., Schubert, E. K., Pham, P., Lewellen, B., and Mankoff, D. A. (2003) SUV varies with time after injection in (18)F-FDG PET of breast cancer: characterization and method to adjust for time differences. *J. Nucl. Med.* **44,** 1044–1050
10. Kissane, J. M., and Robins, E. (1958) The fluorometric measurement of deoxyribonucleic acid in animal tissues with special reference to the central nervous system. *J. Biol. Chem.* **233,** 184–188
11. Paroder-Belenitsky, M., Maestas, M. J., Dohan, O., Nicola, J. P., Reyna-Neyra, A., Follenzi, A., Dadachova, E., Eskandari, S., Amzel, L. M., and Carrasco, N. (2011) Mechanism of anion selectivity and stoichiometry of the Na^+/I- symporter (NIS). *Proc. Natl. Acad. Sci. U. S. A.* **108,** 17933–17938
12. Dai, G., Levy, O., and Carrasco, N. (1996) Cloning and characterization of the thyroid iodide transporter. *Nature* **379,** 458–460
13. Ris-Stalpers, C. (2006) Physiology and pathophysiology of the DUOXes. *Antioxid. Redox Signal.* **8,** 1563–1572
14. Dadachova, E., and Carrasco, N. (2004) The Na/I symporter (NIS): imaging and therapeutic applications. *Semin. Nucl. Med.* **34,** 23–31
15. Dohan, O., Portulano, C., Basquin, C., Reyna-Neyra, A., Amzel, L. M., and Carrasco, N. (2007) The Na^+/I symporter (NIS) mediates electroneutral active transport of the environmental pollutant perchlorate. *Proc. Natl. Acad. Sci. U. S. A.* **104,** 20250–20255
16. Takeuchi, K., Suzuki, H., Horiuchi, Y., and Mashimo, K. (1970) Significance of iodide-perchlorate discharge test for detection of iodine organification defect of the thyroid. *J. Clin. Endocrinol. Metab.* **31,** 144–146
17. Engler, H., Taurog, A., and Dorris, M. L. (1982) Preferential inhibition of thyroxine and 3,5,3′-triiodothyronine formation by propylthiouracil and methylmercaptoimidazole in thyroid peroxidase-catalyzed iodination of thyroglobulin. *Endocrinology* **110,** 190–197
18. McDonald, D. O., and Pearce, S. H. (2009) Thyroid peroxidase forms thionamide-sensitive homodimers: relevance for immunomodulation of thyroid autoimmunity. *J. Mol. Med. (Berl.)* **87,** 971–980
19. Dedek, K., and Waldegger, S. (2001) Colocalization of KCNQ1/KCNE channel subunits in the mouse gastrointestinal tract. *Pflügers Arch.* **442,** 896–902
20. Geibel, J. P. (2005) Role of potassium in acid secretion. *World J. Gastroenterol.* **11,** 5259–5265
21. Roepke, T. K., Kanda, V. A., Purtell, K., King, E. C., Lerner, D. J., and Abbott, G. W. (2011) KCNE2 forms potassium channels with KCNA3 and KCNQ1 in the choroid plexus epithelium. *FASEB J.* **25,** 4264–4273

Received for publication February 29, 2012.
Accepted for publication April 16, 2012.